Water in Plagioclase Phenocrysts from the 2009 Eruption of Redoubt Volcano, Alaska

COLLEGE OF COMPUTER, MATHMATICAL, & NATURAL SCIENCES
DEPARTMENT OF GEOLOGY

Robert A. Stutzke (GEOL 394)
Advisors: Dr. Megan E. Newcombe and Sumedha Desikamani

COLLEGE OF COMPUTER, MATHMATICAL, & NATURAL SCIENCES
DEPARTMENT OF GEOLOGY

Introduction

Volcanic eruptions threaten human health and productivity. Accurate eruption forecasting remains a challenge, even in well-monitored volcanic systems. Pre-eruptive geophysical observations understood within a post-eruptive petrologic context may help inform future forecasting efforts by tying pattern recognition to a more mechanistic understanding of magma storage and migration in volcanic systems. This project tested a method to use the water in plagioclase hygrometer to estimate pre-eruptive magma storage depths of two 2009 Redoubt eruption Events. These depths were then compared to other petrologic and geophysical estimations of magma storage and migration.

Hypothesis

Storage depths calculated from water-in-plagioclase will overlap within uncertainty with existing storage depths estimated from plagioclase-melt hygrometry and pre-eruptive earthquake hypocenter depths.

Methods

Figure 1: Sample Preparation (A), FTIR Spot Analysis (B), and Area Baseline Picks (C,D)
Plagioclase grains are mounted, cut, and polished. One spot is analyzed by FTIR. Two linear baselines are drawn to define a lower and upper bound of OH^- peak expression.

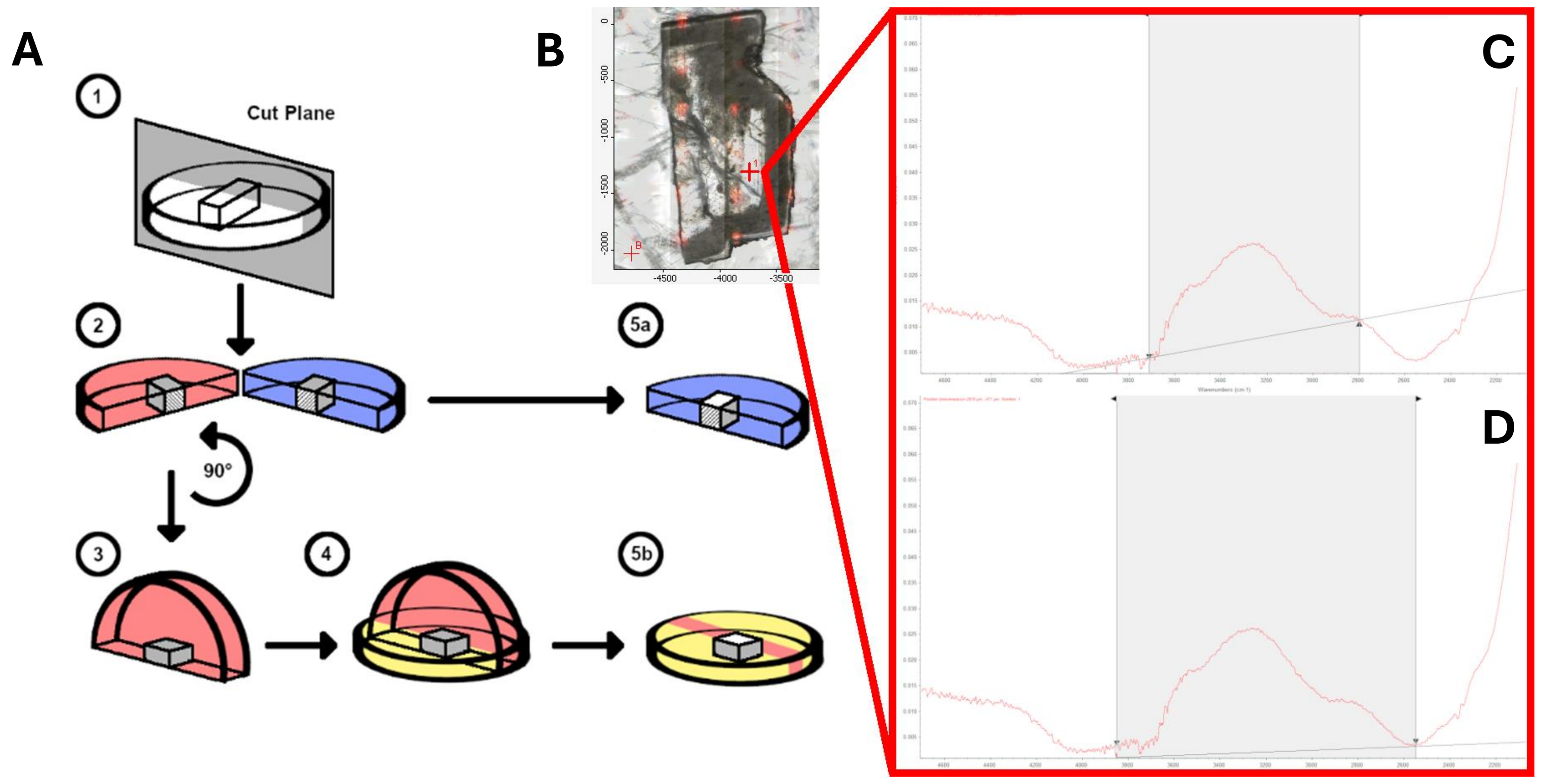

Figure 2: Polarization and Area Calculation
Two spectra polarized at 0° and 90° were taken per spot. Absorbance area for cut slabs was calculated by Method 1. Absorbance area for single slabs was calculated by Method 2 and Method 3. Methods were compared.

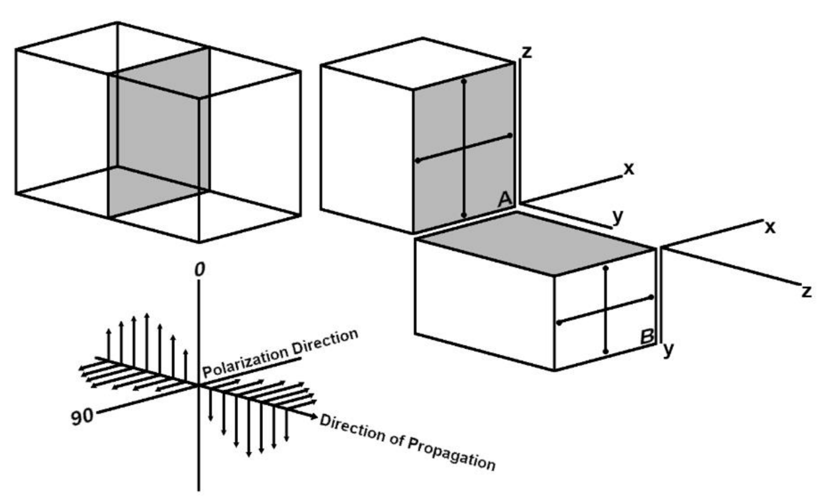

Method 1 $$A_{tot} = A_x + A_y + A_z$$

Method 2 $$A_{tot} = \frac{3}{2}(A_x + A_y)$$

Method 3 $$A_{tot} = A_x + 2A_y \ \ where\ A_x > A_y$$

Sample	Estimate Type	Method 1 vs. Method 2	Method 1 vs. Method 3	Method 2 vs. Method 3
E5C4 – X1 – H1	Upper Estimate (ppm)	6	0	6
	Lower Estimate (ppm)	1	2	3
E5C4 – X1 – H2	Upper Estimate (ppm)	14	0	14
	Lower Estimate (ppm)	9	2	9

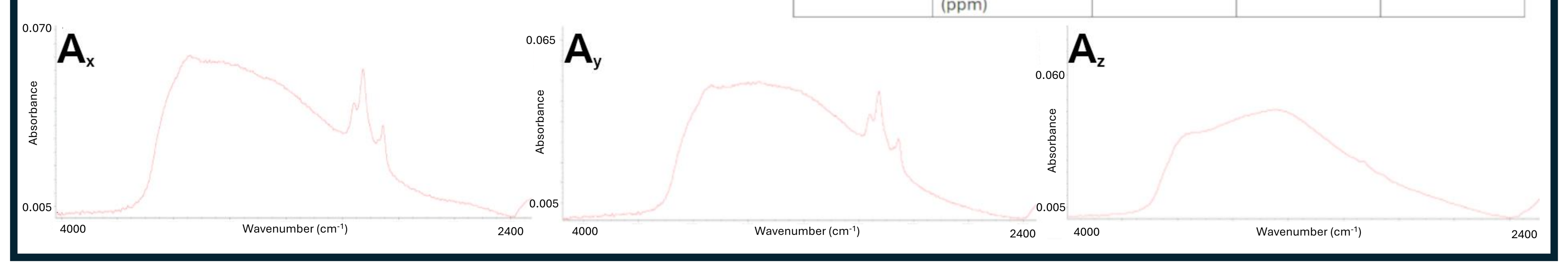

Methods Continued

Figure 3: Water Concentration to Depth
Water concentration (C; wt % H_2O) in the sample may be calculated by the Beer-Lambert Law using absorbance area (A; cm^{-1}). H_2O concentration in the melt is related to H_2O concentration in the crystal using a plagioclase-melt partition coefficient (K_d; 0.002 in this study). H_2O concentration in the melt can then be related to a confining pressure (P) through VolatileCalc. A depth (h) may then be found.

$$C = \frac{(mw)(A)}{\rho * d * \varepsilon} \longrightarrow C_{melt\ (wt\ \%)} = \frac{C_{crystal\ (wt\ \%)}}{K_d} \longrightarrow \text{VolatileCalc (Newman and Lowenstern, 2002)} \longrightarrow P = \rho g h$$

Results

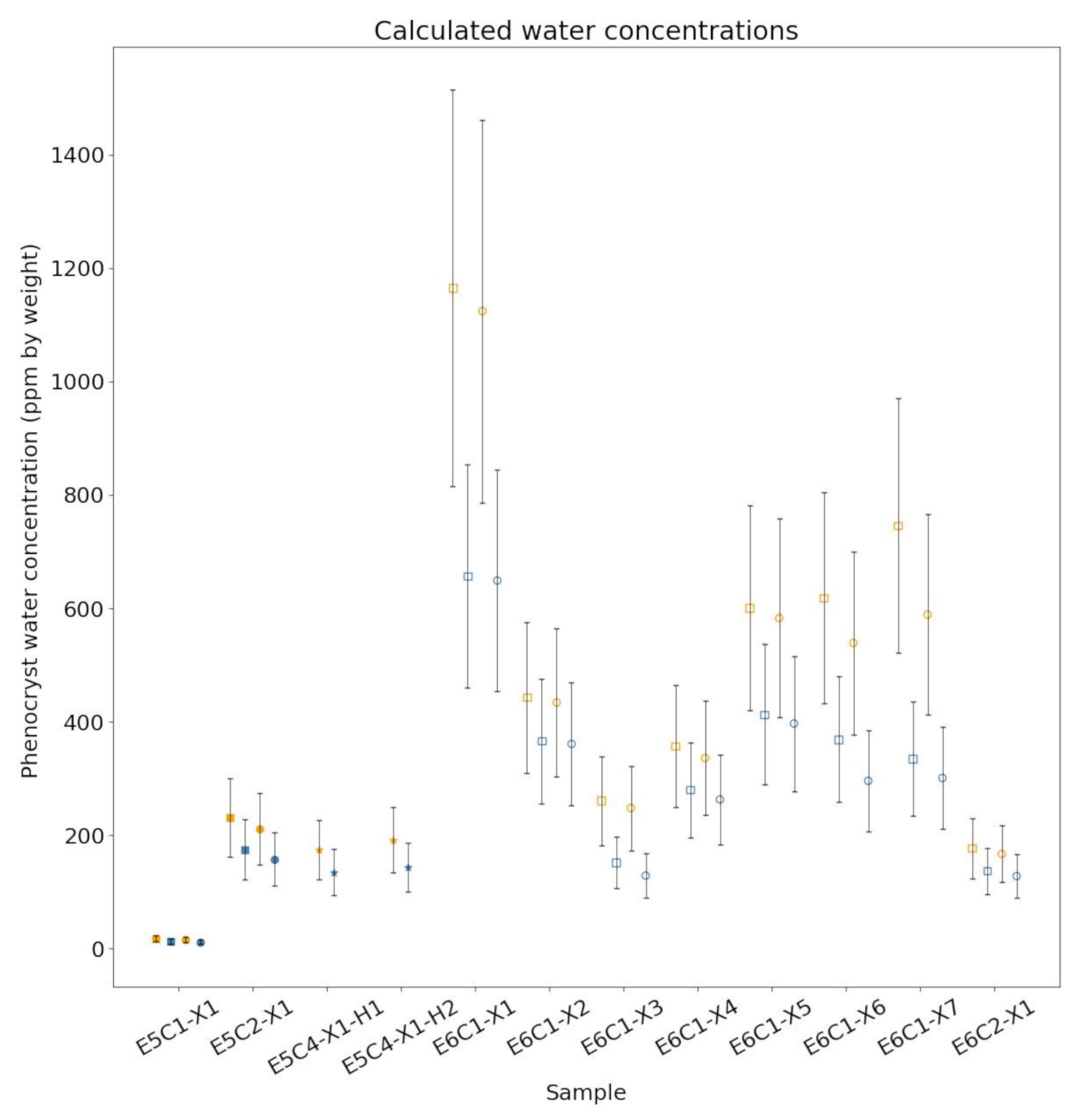

Figure 4: Plotted Calculated Water Concentrations
Orange symbols represent upper estimates. Blue symbols represent lower estimates. Solid symbols represent Event 5 samples. Open symbols represent Event 6 samples. Stars are concentrations calculated using areas determined by Method 1. Squares are concentrations calculated using areas determined by Method 2. Circles are concentrations calculated using areas determined by Method 3. The uncertainty for every sample is ± 30 %.

Figure 5: Complications in Interpretation – Inclusions
Left: (A) Reflected light (x5 optic). (B) Transmitted light (x50 optic). Mineral, melt, and fluid inclusions are present in all samples and may have intersected the IR beam path during measurement. Right: visual (top) and spectral (bottom) identification of inclusions.

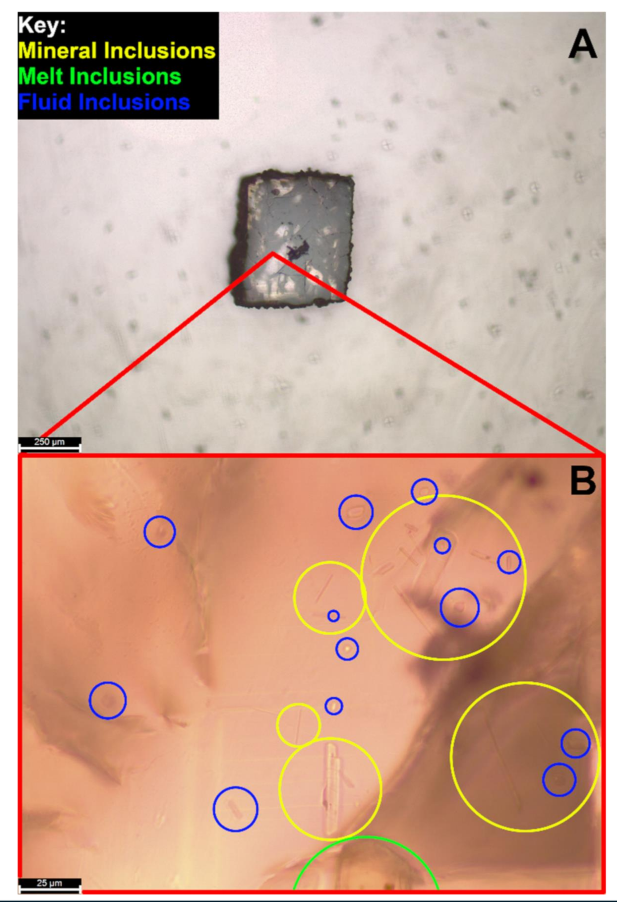

Visually Identified Inclusions

Sample	Fluid Inclusions	Melt Inclusions	Mineral Inclusions
E5C1 – X1	O	X	X
E5C2 – X1	O	?	X
E5C4 – X1 – H1	O	?	?
E5C4 – X1 – H2	O	X	X
E6C1 – X1	O	X	?
E6C1 – X2	O	?	X
E6C1 – X3	O	X	X
E6C1 – X4	O	?	?
E6C1 – X5	O	?	X
E6C1 – X6	O	?	?
E6C1 – X7	O	X	X
E6C2 – X1	O	X	X

Spectrally Identified Inclusions

Split columns for polarization directions 0° and 90°

Sample	Fluid Inclusions**		Melt Inclusions††		Organics‡‡	
E5C1 – X1	?	?	X	X	O	O
E5C2 – X1	?	?	?	X	O	X
E5C4 – X1 – H1	?	?	O	O	O	O
E5C4 – X1 – H2	?	?	X	O	O	O
E6C1 – X1	O	O	X	X	O	O
E6C1 – X2	O	O	X	X	X	X
E6C1 – X3	?	?	?	X	O	X
E6C1 – X4	?	O	X	X	X	X
E6C1 – X5	?	?	X	X	O	O
E6C1 – X6	?	X	?	X	O	X
E6C1 – X7	?	O	?	?	O	O
E6C2 – X1	?	?	X	X	O	O

** Fluid inclusions have a peak at 3450 cm^{-1} and a shoulder at 3270 cm^{-1} (Johnson and Rossman, 2004).
†† Melt inclusions have an asymmetric peak skewed to the right (Johnson and Rossman, 2004).
‡‡ C – H bonds spectrally have three peaks clustered between 3000^{-1} and 2800^{-1} (Johnson and Rossman, 2004).

Results Continued

Figure 6: Compiled Estimations of Magma Storage and Migration Depths
Brown shaded regions indicate geophysical estimations. Purple shaded regions indicate geochemical estimations. The dotted blue line indicates sea level. Redoubt summit peak is ~ 3 km ASL. Sample E5C1 – X1 depth is plotted in comparison. Orange symbols represent upper estimates. Blue symbols represent lower estimates. Squares are concentrations calculated using areas determined by Method 2. Circles are concentrations calculated using areas determined by Method 3.

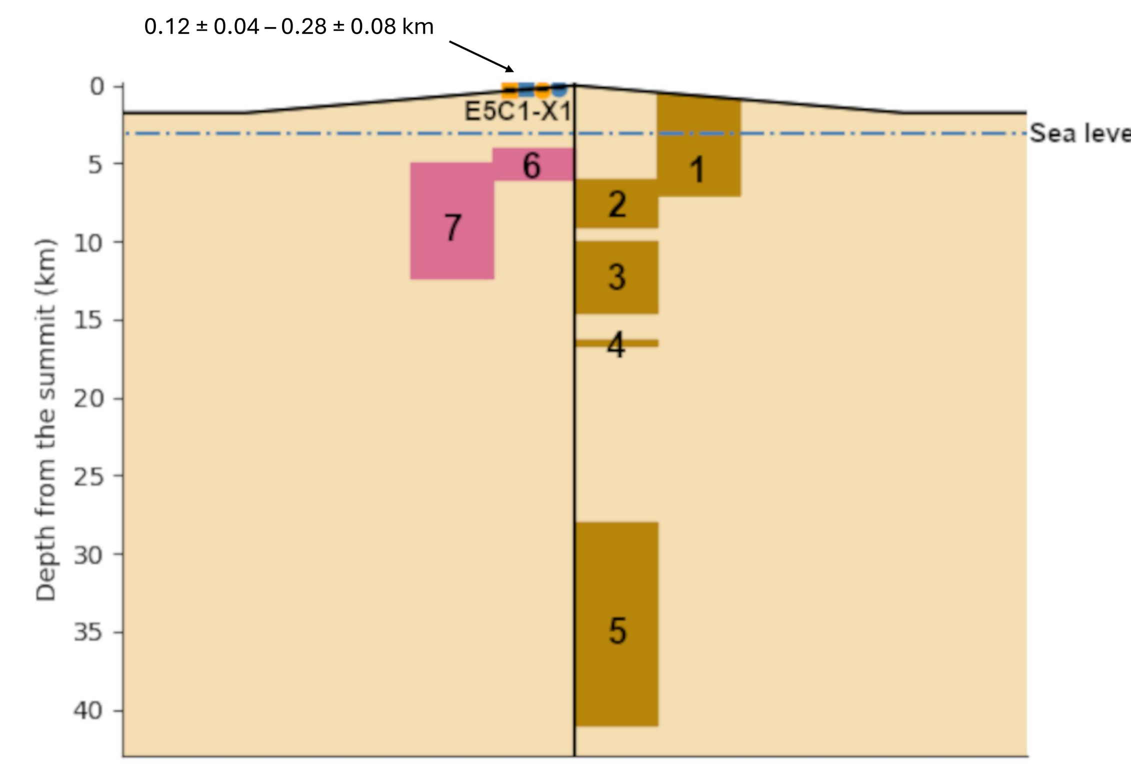

Estimations of Magma Storage and Migration Depths

Label Number	Method	Depth
	Geophysical Estimations	
1	P1 swarm of Mar. 20-23 (Ketner and Power, 2013 for ID and Power et al., 2013 for depths)	0 – 7 km
2	Active magma migration (tremors in 6-week lead-up from late January 2009) (Buurman et al., 2013; Bull & Buurman, 2013)	6 – 9 km
3	Geodesy - Mid-crustal reservoir (Grapenthin et al., 2013)	10 – 14.5 km
4	Geodesy - Deep hot magma injection from > 23 km (Grapenthin et al., 2013)	16.5 km
5	DLPs – Dec. 2008 (Power et al., 2013)	28 – 41 km
	Geochemical Estimations	
6	Pl-melt hygrometry Events 5, 6 (Coombs et al., 2013)	4 – 6 km
7	Pl-hosted MIs Events 5, 6 (Hosseini et al., 2023)	4.9 – 12.3 km

Conclusions

- Calculated plagioclase H_2O concentrations varied from 8.8 ± 2.6 – 1165 ± 350 ppm (1σ). Some of this water was from inclusions and organics. Structurally bound OH^- concentration values are lower than measured values. The plagioclase-melt partition coefficient only applies to structurally bound OH^-.
- Calculated depths ranged from 0.12 ± 0.04 to > 34 km (1σ). True depths are likely shallower.
- The depth ranges generally do not agree with petrologic or geodetic estimations of magma storage depths. There is some agreement with the geophysical record.
- Sample E5C1-X1 likely diffusively re-equilibrated or crystallized within the conduit. As Events 1 – 5 occurred within hours of each other, a deep source plagioclase would likely not have time to re-equilibrate to a low water concentration. This crystal may represent entrained non-juvenile material.
- The plagioclase hygrometer, if applied appropriately, could be a broadly applicable and reliable indicator of host melt water contents.

References and Acknowledgements

Bull, K.F., Buurman, H., 2013. An overview of the 2009 eruption of Redoubt Volcano, Alaska. Journal of Volcanology and Geothermal Research 259, 2–15. https://doi.org/10.1016/j.jvolgeores.2012.06.024

Buurman, H., West, M.E., Thompson, G., 2013. The seismicity of the 2009 Redoubt eruption. Journal of Volcanology and Geothermal Research 259, 16–30. https://doi.org/10.1016/j.jvolgeores.2012.04.024

Coombs, M.L., Sisson, T.W., Bleick, H.A., Henton, S.M., Nye, C.J., Payne, A.L., Cameron, C.E., Larsen, J.F., Wallace, K.L., Bull, K.F., 2013. Andesites of the 2009 eruption of Redoubt Volcano, Alaska. Journal of Volcanology and Geothermal Research 259, 349–372. https://doi.org/10.1016/j.jvolgeores.2012.01.002

Grapenthin, R., Freymueller, J.T., Kaufman, A.M., 2013. Geodetic observations during the 2009 eruption of Redoubt Volcano, Alaska. Journal of Volcanology and Geothermal Research 259, 115–132. https://doi.org/10.1016/j.jvolgeores.2012.04.021

Hosseini, B., Myers, M., Loewen, M., Wieser, P.E., DeVitre, C.L., Wallace, K.L., Coombs, M.L., 2023. Redoubt 2009 Revisited: A Melt Inclusion Perspective on the Source Region of the Low-Silica Andesite, in: AGU Fall Meeting Abstracts. American Geophysical Union, Fall Meeting 2023.

Johnson, E.A., Rossman, G.R., 2004. A survey of hydrous species and concentrations in igneous feldspars. American Mineralogist 89, 586–600.

Ketner, D., Power, J., 2013. Characterization of seismic events during the 2009 eruption of Redoubt Volcano, Alaska. Journal of Volcanology and Geothermal Research 259, 45–62. https://doi.org/10.1016/j.jvolgeores.2012.10.007

Newman, S., Lowenstern, J.B., 2002. VolatileCalc: a silicate melt-H2O-CO2 solution model written in Visual Basic for Excel. Comput Geosci 28, 597–604.

Power, J.A., Stihler, S.D., Chouet, B.A., Haney, M.M., Ketner, D.M., 2013. Seismic observations of Redoubt Volcano, Alaska - 1989-2010 and a conceptual model of the Redoubt magmatic system. Journal of Volcanology and Geothermal Research 259, 31–44. https://doi.org/10.1016/j.jvolgeores.2012.09.014

Thank you to the Alaska Volcano Observatory for providing the Event 5 and Event 6 pyroclast samples used in this study. Thank you to the University of Maryland, Department of Geology for offering the Senior Thesis program. Thank you to my advisors Dr. Megan E. Newcombe and Sumedha Desikamani, the Senior Thesis director Dr. Philip M. Piccoli, and members of the UMD Planetary Volcanism Laboratory for their guidance on this project.